

Analysis and Design of Analog Fountain Codes for Short Packet Communications in IoT

Wen Jun Lim, *Student Member, IEEE*, Mahyar Shirvanimoghaddam, *Senior Member, IEEE*, Rana Abbas, *Member, IEEE*, Yonghui Li, *Fellow, IEEE*, Branka Vucetic *Fellow, IEEE*

Abstract—In this paper, we focus on the design and analysis of the Analog Fountain Code (AFC) for short packet communications. We first propose a density evolution (DE) based framework, which tracks the evolution of the probability density function of the messages exchanged between variable and check nodes of AFC in the belief propagation decoder. Using the proposed DE framework, we formulate an optimisation problem to find the optimal AFC code parameters, including the weight-set, which minimizes the bit error rate at a given signal-to-noise ratio (SNR). Our results show the superiority of our code design in comparison to existing code designs and thus the validity of the proposed DE framework in the asymptotic block length regime. We then focus on the selection of the precoder to improve the performance of AFC at short block lengths. Simulation results show that lower precoder rates obtain better realised rates over a wide SNR range for short information block length.

Index Terms—Analog fountain code (AFC), density evolution, differential evolution optimization, rateless codes.

I. INTRODUCTION

THE third generation partnership project (3GPP) has defined 3 main services for the fifth generation (5G) of mobile communications [1]. These include enhanced mobile broadband (eMBB), ultra-reliable low-latency communications (URLLC), and massive machine type communications (mMTC). 5G aims at providing higher data rate (e.g., up to 10 Gbps for eMBB), shorter end-to-end latency (e.g., ≤ 1 ms for URLLC), and higher energy efficiency (e.g., up to 10 years operation with a single battery for mMTC) [2]. Many new techniques have been proposed to meet these quality of service requirements, e.g., massive multiple-input-multiple-output (mMIMO), millimeter wave (mmW) communications, non-orthogonal multiple access (NOMA), etc. [3], [4]. Amongst these initiatives, the choice of the channel coding techniques remains an essential part to unleash the full potential of 5G New Radio (NR) services, namely, to guarantee the required latency and reliability requirements at maximum efficiency [2].

The design of efficient and robust short packet communications is vital for 5G mMTC and URLLC applications, where the data transferred might be significantly smaller than traditional human-based communications, ranging from a few hundreds bits down to a few tens [5], [6]. In particular, there is

large consensus that traditional channel codes, adopted in current cellular networks, are strictly sub-optimal for short packet communications [7]. Modern channel coding techniques have diverged away from the traditional theories of Shannon, due to this new shift alongside other challenges imposed by the 5G services, e.g., higher reliability requirements (lower than 10^{-5}) and higher energy efficiency. We refer the readers to the survey paper in [7] for a comprehensive review of modern channel coding techniques. Amongst the proposed techniques, the 3GPP Release-15 standard [1] has indicated that eMBB will be using low density parity check (LDPC) codes in the data channels and Polar codes in the control channels [8]. Currently, the standardisation of the channel coding techniques for URLLC and mMTC is still underway [9].

In this paper, we focus on modern rateless codes as a potential candidate for 5G. When employing fixed-rate channel codes, rate adaptation to the varying wireless channel requires the receiver to frequently feedback channel state information to the transmitter to select the best coding and modulation scheme. For short block lengths, the overhead incurred by this feedback can be costly both in terms of spectrum efficiency for mMTC and in terms of latency for URLLC [10]. This is where self-adaptive codes, also known as rateless codes, come in as an attractive candidate. In rateless codes, the rate is determined on-the-fly without the need for the transmitter to be aware of the channel conditions. This is particularly favourable in fast varying channels as well as non-reciprocal channels.

A. Related Works

The original research on rateless codes, such as LT codes [11] and Raptor codes [12], have shown that rateless code can achieve the channel capacity over binary erasure channels. A modified version of Raptor codes, called RaptorQ, has been standardised for mobile wireless communication broadcast and multicast, as well as DVB-H standards for IP datacast [13]. However, all design extensions of rateless codes to noisy channels, e.g., additive white Gaussian noise (AWGN) channel, have shown to be channel dependent. To the best of our knowledge, only a few rateless codes to date are near capacity-achieving over a wide range of SNRs for an asymptotically long block length, such as analog fountain codes [14] and Spinal codes [15]. This gap to the capacity is significantly degraded for short block lengths [5]. The application of short rateless codes in 5G NR services has been demonstrated in several works, including protograph-based raptor-like LDPC codes in [16], which showed satisfactory

This paper was presented in part at the IEEE 90th Vehicular Technology Conference, Honolulu, HI, USA, Sep. 2019.

The authors are with the Centre for IoT and Telecommunications, School of Electrical and Information Engineering, The University of Sydney, NSW 2006, Australia (e-mail: {wenjun.lim; mahyar.shirvanimoghaddam; rana.abbas; yonghui.li; branka.vucetic}@sydney.edu.au).

performance in the short block length regime. Meanwhile, the research carried out in [17] identified the challenges for the design of channel codes to address the specification of mMTC, and the work in [18] proposed bi-interleave coded multiple access (BICMA) as a multiple access scheme in the physical layer of mMTC, where it can support high demanding load with high energy efficiency and low complexity. Although these works demonstrated good performance of short rateless codes for mMTC application, the underlying rateless codes are mainly binary and heavily dependent on SNR. On the other hand, the research in [19] evaluates the techniques in physical layer and MAC layer to increase reliability and reduce latency, and provide numerical evaluation of URLLC which is enabled by coexistence of LTE in unlicensed spectrum. The work carried out in [20], [21] demonstrated guideline for Rate Compatible Modulation (RCM) in selection of weights according to channel condition for reduced complexity without loss of performance and also parallel belief propagation (BP), respectively. However, the proposed designs therein were mostly heuristic and did not provide meaningful insights into the code design for short block lengths.

Recent results on short AFC [22] have shown impressive results for 5G URLLC in terms of comparable latency to the Polyanskiy-Poor and Verdu (PPV) normal approximation [23] as well as reliability down to 10^{-7} . However, the proposed encoding scheme therein as well as the weight set design are based on heuristics rather than a solid analytical framework. In this paper, we aim to bridge this gap in the literature by providing a solid analytical framework as well as an optimisation framework for AFC. To the best of our knowledge, the only work that has attempted to do so can be found in [24]. Authors in [24] proposed a modified weight selection scheme for short block length weight-adaption AFC (SWA-AFC), which achieves significant coding gains, close to the PPV bound. In particular, the extrinsic information transfer (EXIT) chart analysis [25] was modified in [24], to address the issue of performance degradation of EXIT analysis in the finite block length regime. The design in [24], however, relies on approximate densities and the assumption of symmetric Gaussian distribution for the messages exchanged in each iteration of the message passing decoder. These assumptions are not accurate [26], particularly at low rates, which negatively impact the search for the optimal code ensembles.

In this work, we employ the density evolution (DE) analysis to track the evolution of the probability distribution function (pdf) of messages exchanged between the nodes in each iteration of the belief propagation (BP) decoding algorithm. DE was previously used in [26] to analyse Raptor codes as a multi-edge type LDPC code. The degree distribution of the Raptor code was then optimized using this framework, which significantly outperformed existing Raptor codes mainly designed using linear programming based on approximate DE algorithms [27] or Gaussian approximations [28], [29]. In what follows, we explain our main contributions in this work.

B. Main Contributions

1) *A Density Evolution-based Framework to Analyse AFC:* A DE framework is proposed in this work to analyse the

performance of the iterative message-passing decoder of AFC. The algorithm is designed in the way to track the evolution of pdf of log-likelihood ratios (LLR) which are exchanged between variable and check nodes during the belief propagation decoding. Due to the complexity of the variable and check node updating rules, we proposed a Monte-Carlo based analysis to derived the pdfs in each iteration of DE. Our results show that the proposed DE framework can precisely approximate the pdf of LLRs in each iteration of BP.

2) *A Differential Evolution Algorithm to Optimize AFC parameters:* We propose an optimization problem based on the DE analysis to find the optimal weight set of AFC. We use differential evolution to solve the optimization problem and find the optimal weight set for AFC with different degrees. Simulation results showed that by applying the optimized weight set, the performance of the AFC is improved regardless in asymptotic long block length and finite block length regime, thus proving the validity of the DE framework proposed.

3) *AFC optimization in the short block length regime:* To further enhance the performance of AFC at short block lengths, we evaluate different precoders with different code rates. In particular, we consider BCH codes with an ordered statistics decoder (OSD) [30] and LDPC codes with BP decoder. The combined code is simulated under different channel conditions where we show that a low rate precoder, offers better reliability at a wide range of SNRs compared to high-rate precoders. We also show that the precoded AFC performs close to the normal approximation benchmark [23] in the finite block length regime over a wide range of SNRs.

C. Paper Organization

The rest of the paper is organized as follows. In Section II, we explain the encoder and decoder of the concatenated AFC code. We then propose the density evolution framework for the analysis and design of AFC in Section III. Section IV presents the differential evolution optimization framework for the AFC weight-set optimization. The design of AFC codes in the short block length will be studies in Section V. Finally, conclusions are drawn in Section VI.

II. ANALOG FOUNTAIN CODES

AFC was originally proposed in [14], which is mainly characterized by a weight set, degree distribution function, and the message length. AFC has linear-complexity encoding and decoding processes in terms of the block length. The code is rateless in nature and can generate a potentially limitless number of coded symbols; thus, achieving any desired rate on-the-fly. In what follows, we explain the encoding and decoding processes of AFC.

A. The Encoder

The precoded AFC is a concatenation of a fixed-rate precode and the AFC code. An information block of length k bits, denoted by \mathbf{b} , is first encoded by using a fixed-rate (n, k) code of rate $R_{\text{pre}} = k/n$, to generate a codeword of length n bits, denoted by \mathbf{u} , referred to as *intermediate symbols*. The

generator matrix of the fixed-rate code is denoted by G_{pre} ; therefore, we have:

$$\mathbf{u} = G_{\text{pre}} \mathbf{b}. \quad (1)$$

The precode serves as the outer code for the precoded AFC code. Intermediate symbols are then modulated by using a BPSK modulation, to generate n modulated symbols, v_i , that is

$$v_i = (-1)^{u_i}, \quad \text{for } i = 1, \dots, n. \quad (2)$$

Next, by using an AFC code a potentially limitless number of AFC coded symbols, also referred to as *output symbols*, are generated. AFC is mainly characterized by a weight set \mathcal{W} and a degree distribution function $\Omega(x) = \sum_{i=1}^n \Omega_i x^i$. In order to generate an AFC coded symbol, a degree d is drawn based on the degree distribution function $\Omega(x)$. Then d modulated intermediate symbols are randomly selected and linearly combined in the real domain with a set of d real weight coefficients selected from the weight set \mathcal{W} . For simplicity, we consider that the degree d is fixed, i.e., $\Omega(x) = x^d$, and the weight set is predefined and given by $\mathcal{W} = \{w_1, w_2, \dots, w_d\}$. The i th AFC coded symbol, denoted by c_i , is then given by:

$$c_i = \sum_{j=1}^d w_j v_{i,j}, \quad (3)$$

where $v_{i,j} \in \mathcal{V}_i$ and \mathcal{V}_i is the set of modulated intermediate symbols that have been chosen to generate the i th output symbol. We further assume that $\sum_{i=1}^d w_i^2 = 1$, therefore we have $\mathbb{E}[|c|^2] = 1$, where $\mathbb{E}[\cdot]$ is the expectation operand. Fig. 1 shows the bipartite graph representation of the AFC code truncated at length m . We refer to AFC coded symbols and intermediate symbols in the bipartite graph of AFC by check and variable nodes, respectively. The degree of a check (variable) node is defined as the number of variable (check) nodes connected to it in the bipartite graph. A regular AFC has constant variable node degree d_v and check node degree d_c .

AFC coded symbols are sent over the channel. Once the receiver received m_0 symbols, it performs the decoding. If the decoding failed, it collects δ additional AFC coded symbols and run the decoder again. This process will continue until the decoding succeeds. The realize rate of the precoded AFC is given by

$$\mathcal{R} = \frac{k}{\mathbb{E}[m_s]} = R_{\text{pre}} \times \frac{n}{\mathbb{E}[m_s]}, \quad (4)$$

where m_s is the number of AFC coded symbols collected to perform a successful decoding.

B. The Decoder

We consider the additive Gaussian noise (AWGN) channel, where the channel output y_i is given by

$$y_i = c_i + n_i, \quad \text{for } i = 1, 2, \dots, \quad (5)$$

where n_i is AWGN with zero mean and variance σ^2 . The signal-to-noise ratio (SNR), denoted by γ , is then given by $\gamma = 1/\sigma^2$.

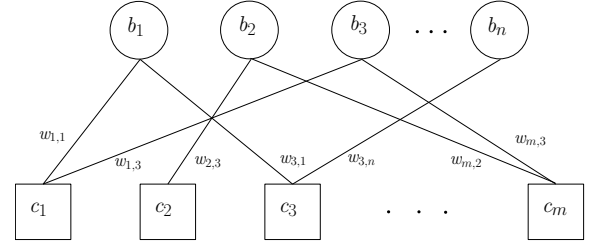


Fig. 1. Bipartite graph representation of an AFC code.

The decoding is performed in two stages. First, the BP decoding algorithm is applied to AFC to find the log-likelihood ratios (LLRs) of intermediate symbols. We use the BP algorithm originally proposed in [31] and further modified in [32] to decode AFC. Second, the LLRs are passed to the decoder of the precode to find the original k information symbols. If the decoding failed, the BP decoding is repeated with a longer block of AFC symbols which includes newly arrived symbols. The LLRs are passed again to the decoder of the precode. This continues until the decoding succeeded or the maximum number of AFC symbols are sent. In this paper, we consider both Bose, Chaudhuri, and Hocquenghem (BCH) codes and LDPC codes as the precode. BCH code is a powerful cyclic error correcting code with a variety of block lengths and corresponding code rates [7]. BCH codes have strong error correcting capability which can correct all random patterns of t errors, where t is the design parameter. BCH codes are effective on preventing error floor due to the large minimum Hamming distance [7]. However there is a shortcoming of BCH codes, which is not flexible enough due to the fact that block length and information length cannot be selected arbitrarily. For BCH precoded AFC, we use the ordered statistics decoder (OSD), which is computationally complex. LDPC on the other hand offers a lower complexity decoder, as BP can be effectively used to decode them. LDPC however cannot offer the same level of error correction capability as BCH codes, particularly at short block lengths.

III. THE DENSITY EVOLUTION ANALYSIS OF AFC

Density Evolution (DE) [33] is a powerful tool used to analyse the belief propagation algorithm and has been extensively applied to graph-based codes with static uniformity. In a nutshell, this technique involves tracking the distribution of the messages exchanged along the edges of the bipartite graph in each iteration of the message passing algorithm (MPA) [34]. In this section, we first rephrase the message passing decoder for AFC and provide a modification to AFC in order to meet the requirement for DE. We then present the updating rules at the variable and check nodes of the bipartite graph of AFC and explain how we implement it in a practical manner.

A. The Message Passing Decoding of AFC

We consider a regular AFC with constant variable and check node degree, d_v and d_c , respectively. In each iteration of MPA (i.e., the BP decoder), messages are exchanged between the check and variable nodes and vice versa. We use the log-likelihood ratio (LLR) as the message which is exchanged between nodes in each iteration of MPA.

Let $m_{c \rightarrow v}^{(\ell)}(w_v)$ denote the message sent from check node c to variable node v along the edge with weight w_v in the ℓ th iteration of MPA. It can be calculated as follows:

$$m_{c \rightarrow v}^{(\ell)}(w_v) = \ln \frac{\sum_{\substack{b_{v'} \in \{-1, 1\} \\ v' \in \mathcal{M}_c \setminus v}} e^{-\frac{\left(y - w_v - \sum_{v' \in \mathcal{M}_c \setminus v} w_{v'} b_{v'}\right)^2}{2\sigma^2}} \prod_{v' \in \mathcal{M}_c \setminus v} p_{v' \rightarrow c}^{(\ell-1)}(b_{v'})}{\sum_{\substack{b_{v'} \in \{-1, 1\} \\ v' \in \mathcal{M}_c \setminus v}} e^{-\frac{\left(y + w_v - \sum_{v' \in \mathcal{M}_c \setminus v} w_{v'} b_{v'}\right)^2}{2\sigma^2}} \prod_{v' \in \mathcal{M}_c \setminus v} p_{v' \rightarrow c}^{(\ell-1)}(b_{v'})}, \quad (6)$$

where $y = c + n$ is the received signal corresponds to check node c , $\mathcal{M}_c \setminus v$ denote the set of variable node connected to check node c except variable node v and

$$p_{v' \rightarrow c}^{(\ell)}(b_{v'}) = \begin{cases} \left(1 + e^{-m_{v' \rightarrow c}^{(\ell)}}\right)^{-1}, & \text{if } b_{v'} = 1, \\ \left(1 + e^{m_{v' \rightarrow c}^{(\ell)}}\right)^{-1}, & \text{if } b_{v'} = -1, \end{cases} \quad (7)$$

and $m_{v \rightarrow c}^{(\ell)}$ denote be the message sent from a variable node v to check node c in the ℓ th iteration of MPA, which is given by

$$m_{v \rightarrow c}^{(\ell)} = \sum_{c' \in \mathcal{N}_v \setminus c} m_{c' \rightarrow v}^{(\ell-1)}(w_{v'}) \quad (8)$$

where $\mathcal{N}_v \setminus c$ represents the set of check nodes that are connected to variable node v except check node c .

The messages are exchanged in an iterative manner between variable and check nodes for a predefined number of iterations or until the decoding achieves convergence. The final LLR value of each variable node after L iterations of MPA is calculated as follows:

$$m_v^{(L)} = \sum_{c \in \mathcal{N}_v} m_{c \rightarrow v}^{(L)}(w_v). \quad (9)$$

These LLRs are then passed to the decoder of the precode to find the original k information symbols.

B. The Density Evolution Analysis

Without loss of generality, we assume that all incoming messages in a node are independent and identically distributed (i.i.d). This assumption was first considered in [33] and further justified in [35]. Based on this assumption, the bipartite graph can be viewed as a set of independent sub-trees with independently distributed messages, making the analysis more feasible. With probability arbitrarily approaching to 1 when n goes to infinity, a cycle-free bipartite graph emerged [35].

The other assumption which has been widely considered for the DE analysis, is the all-zero codeword transmission. For this condition to be met, the output channel LLRs should be symmetric that is the bit error rate is independent of the transmitted codeword [36]. However, AFC does not meet this condition as the average power of the output symbols depends on the information sequence. For example, when the all-zero

information sequence is being encoded using AFC, each coded symbol will be equal to $\sum_{i=1}^d w_i$ which is equivalent to the signal with the highest power assuming that w_i 's are all positive. For an information sequences with some non-zero symbols, some of the coded symbols will have lower power. This results in an unequal protection of information sequences. To solve this problem and meet the requirements for the DE analysis, we adopt the idea of the independent and identically distributed (i.i.d) channel adapter [37].

In particular, we slightly modify the encoding process of AFC in (3) by multiplying a binary random number, i.e., $+1$ and -1 , with the weight associated to each edge in the bipartite graph. The i th AFC coded symbols is then generated as follows:

$$c_i = \sum_{j=1}^d (-1)^{t_j} w_j v_{i,j}, \quad (10)$$

where t_j 's are uniformly and randomly drawn from set $\{0, 1\}$. In the rest of the paper, we use this modified encoder unless otherwise specified.

1) DE Check Node Updating Rule: It is important to note that unlike binary graph-based codes which are mainly characterized by the degree distribution function in the asymptotic block length regime, the analysis of AFC should also take into account the weights associated with each edge in the graph. To do so, we assume that the messages passed from check to variable nodes are weight dependent. Let $m_{c \rightarrow v}^{(\ell)}(w)$ denote the message passed from check node c to variable node v along the edge with weight w in the ℓ th iteration of MPA. Let $f_{cv}^{(\ell)}(w, m)$ denote the pdf of $m_{c \rightarrow v}^{(\ell)}(w)$. In DE, we track the evolution of $f_{cv}^{(\ell)}(w, m)$.

To calculate $f_{cv}^{(\ell)}(w, m)$, we need to find the pdf of $m_{c \rightarrow v}^{(\ell)}(w)$ which is derived in (6). Due to the complexity of this equation, it is not straightforward to find $f_{cv}^{(\ell)}(w, m)$. To address this, we propose to collect the exchanged messages by random sampling, i.e., by performing Monte-Carlo simulations. In particular, we randomly generate samples of y assuming that an all zero-codeword is being sent. It is important to note that for DE we consider channel adapters and therefore the modified encoder in (10). We also randomly generate samples of $p_{v \rightarrow c}^{(\ell-1)}(b_v)$ from the pdf of $m_{v \rightarrow c}^{(\ell-1)}$, denoted by $f_{vc}^{(\ell-1)}(m)$.

More specifically, to generate samples of $p_{v \rightarrow c}^{(\ell-1)}(b_v)$, we first draw a random number $m_{v \rightarrow c}^{(\ell-1)}$ from $f_{vc}^{(\ell-1)}(m)$. Then by using (7), $p_{v \rightarrow c}^{(\ell-1)}(b_v)$ is calculated for $b_v = 1$ and $b_v = -1$. These will be inserted into (6) to calculate one sample of $m_{c \rightarrow v}^{(\ell)}(w)$. Once a large number of samples are generated, $f_{cv}^{(\ell)}(w, m)$ can be approximated by finding the histogram of samples of $m_{c \rightarrow v}^{(\ell)}(w)$.

2) DE Variable Node Updating Rule: Let $f_{vc}^{(\ell)}(m)$ denote the pdf of the $m_{v \rightarrow c}^{(\ell)}$, which is given in (8). As we assume that the messages passed along the edges are independent in an asymptotic long block length regime, we can find $f_{vc}^{(\ell)}(m)$

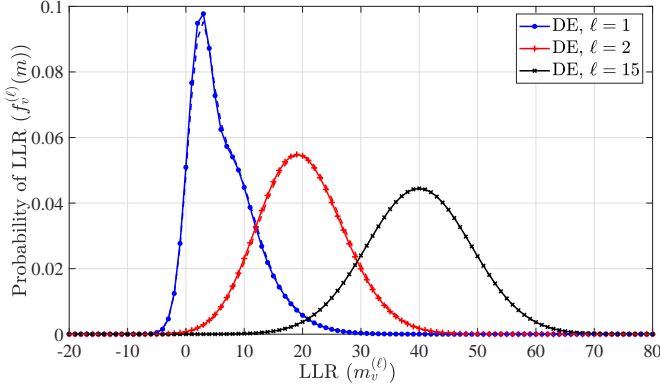


Fig. 2. The variable node densities calculated by DE at different decoding iterations for an AFC code with information length $n = 8000$, weight set $\mathcal{W} = \{0.5097, 0.4992, 0.4960, 0.4949\}$, check node degree $d_c = 4$, and rate $R = 0.5$, when SNR = 10dB. Solid and dashed curves respectively show DE analytical results and simulation results.

as follows:

$$f_{vc}^{(\ell)}(m) = \frac{1}{2d_c} \bigotimes_{i=1}^{d_v-1} \bigotimes_{w \in \mathcal{W}^\pm} f_{cv}^{(\ell)}(w, m), \quad (11)$$

where $\mathcal{W}^\pm = \{w, -w : w \in \mathcal{W}\}$ is the set of all positive and negative weight coefficients due to channel adapter. This equation follows from the fact that each variable node has d_v connected check nodes and the edges have weights which are randomly drawn from \mathcal{W}^\pm . Since each edge can randomly choose one of the $2d_c$ available weight coefficients, we normalize the density by multiplying it with $\frac{1}{2d_c}$. Fig. 2 shows the densities $m_v^{(\ell)}$ at different iterations of MPA for an AFC code with weight set $\mathcal{W} = \{0.5097, 0.4992, 0.4960, 0.4949\}$, degree $d_c = 4$, and rate $R = 0.5$, when SNR = 10dB. As can be seen in this figure, the densities are shifting towards right when the iteration number increases.

3) *Approximation of the bit error rate using DE:* We assume that DE converges after a few iterations and the check to variable node densities converge to $f_{cv}^{(\infty)}(w, m)$. The variable node density denoted by $f_v^{(\infty)}(m)$ is then given by:

$$f_v^{(\infty)}(m) = \frac{1}{2d_c} \bigotimes_{i=1}^{d_v} \bigotimes_{w \in \mathcal{W}^\pm} f_{cv}^{(\infty)}(w, m), \quad (12)$$

The bit error rate (BER) of the AFC code, denoted by $\epsilon(d_c, d_v, \mathcal{W})$, can then be calculated as follows:

$$\epsilon(d_c, d_v, \mathcal{W}) = \int_{-\infty}^0 f_v^{(\infty)}(x) dx, \quad (13)$$

which directly follows from the assumption of all-zero information sequence and that a bit error occurs when the LLR is calculated to be negative. Fig. 3 shows the approximation of BER at different decoding iterations using the DE analysis for an AFC code at different SNRs when $n = 8000$. As can be seen, (13) provides a tight approximation for the BER for AFC codes when the information block length n is large.

IV. AFC WEIGHT SET OPTIMISATION

In this section, we use the DE analysis and define an optimization problem to minimize the bit error rate of the

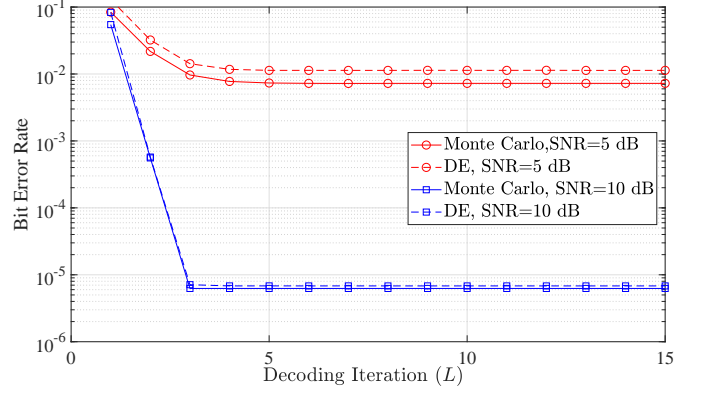


Fig. 3. The BER of AFC at different decoding iterations with the information length $n = 8000$, check node degree $d_c = 4$, weight set $\mathcal{W} = \{0.8632, 0.4495, 0.2300, 0.0004831\}$, and rate $R = 0.5$

AFC and find the optimal weight set for a given check node degree d_c , variable node degree d_v , and channel SNR. The optimization problem can be summarized as follows:

$$\begin{aligned} \min_{\mathcal{W}} \quad & \epsilon(d_c, d_v, \mathcal{W}) \\ \text{s.t.} \quad & C_1 : w_i > 0, \text{ for } i = 1, \dots, d_c, \\ & C_2 : \sum_{i=1}^{d_c} w_i^2 \approx 1, \end{aligned} \quad (14)$$

where (14) is found via (13), condition C_1 is to make sure that all weight coefficients are positive, and condition C_2 it to make sure the average power of the AFC coded symbols is 1. Traditionally, the optimization of a graph-based channel codes involved maximizing the decoding threshold. This is equivalent to minimizing the bit error rate, which we consider in this paper for AFC. We further note that we are interested in finding the optimal weight set for a given fixed code degree d_c . A more general optimization can be easily defined to jointly determine the optimal degree distribution function and weight set. This is however out of the scope of this paper.

We use the differential evolution algorithm [38] to solve (14). The differential evolution is a simple yet powerful optimization tool based on the population stochastic search technique. There are three main parameters that control the optimization algorithm, which include, the scaling factor, crossover probability, and population size. The setting of these three parameters would directly affect the time and performance of the optimization process. The population of differential evolution may move through different region of search space to find suitable candidates. Although this approach is time consuming, it suffices our purpose as we do not aim for efficient optimization and instead would like to find some good weight sets for AFC.

For the case of AFC, the optimization process involved the tuning of weight-set with prefixed rate at the given SNR to minimize the BER as in (14). Table I shows the optimized AFC weight set for different degree d_c , when the rate is $R_{\text{AFC}} = 2$ and SNR is 15 dB. In this optimization, we performed 100 iterations of the density evolution and generate 1000 samples of LLRs to calculate the densities in (11). As

TABLE I
OPTIMISED WEIGHT SETS OBTAINED BY (14), FOR AFC AT SNR= 15dB
WHEN $R_{\text{AFC}} = 2$.

	d_c	Weight Set
\mathcal{W}_1	2	{0.7202, 0.6938}
\mathcal{W}_2	3	{0.7050, 0.5234, 0.4786}
\mathcal{W}_3	4	{0.8632, 0.4495, 0.2300, 0.0004831}
\mathcal{W}_4	5	{0.7272, 0.5014, 0.3151, 0.2921, 0.0754}
\mathcal{W}_5	6	{0.8006, 0.4914, 0.2357, 0.1802, 0.1713, 0.0174}
\mathcal{W}_6	7	{0.7846, 0.4197, 0.4023, 0.1522, 0.1151, 0.0739, 0.0676}

TABLE II
BENCHMARK WEIGHT SETS IN THE LITERATURE FOR AFC WHEN $d_c = 4$.

Name	Weight Set
\mathcal{V}_1 [14]	{0.9103, 0.3641, 0.1655, 0.1071}
\mathcal{V}_2 [14]	{0.8902, 0.3815, 0.2054, 0.1406}
\mathcal{V}_3 [24]	{0.7303, 0.5477, 0.3651, 0.1826}
\mathcal{V}_4 [32]	{0.6576, 0.6576, 0.3288, 0.1644}

for the differential evolution, we considered the population size of approximately 50, crossover probability of 1, and mutation factor of 0.85.

When optimizing the weight set of the AFC using (14), we need to specify the rate and SNR. In other words, the weight set obtained through (14) depend on the rate and channel SNR. For example, when $R_{\text{AFC}} = 0.5$ and $\gamma = 5\text{dB}$, the optimised weight set we obtained for $d_c = 4$ is $\mathcal{W}_3^* = \{0.5097, 0.4992, 0.4960, 0.4949\}$. When $R_{\text{AFC}} = 2$ and $\gamma = 15\text{dB}$, the optimised weight set we obtained for $d_c = 4$ will be $\mathcal{W} = \{0.8632, 0.4495, 0.2300, 0.0004831\}$. The optimized weight coefficients seem to be closer to each other when optimizing AFC at lower SNRs and rates.

Fig. 4 compares the BER performance of AFC with these two weight sets when $R_{\text{AFC}} = 0.5$. As can be seen, the weight set optimised at higher SNR and higher rate performs better compared to weight set optimised at a low SNR and low rate. This observation provide us a guideline on the input parameter selection for the optimisation process, i.e., the rate and SNR should be as high as possible within the region of investigation in order to obtain better performance. We also compared the optimized weight sets with with some weight sets which were previously used in the literature (see Table II) [14], [24], [32]. Fig.4 shows the superiority of the optimized weight sets for AFC in terms of BER.

V. DESIGN OF AFC FOR SHORT PACKET COMMUNICATIONS

In this section, we evaluate the precoded AFC in the short block length regime. The main focus of this section would be determining the precode, where we specifically focus on BCH codes for very short block lengths and LDPC codes for moderate to long block lengths.

We use the normal approximation [23] developed by Polyanskiy-Poor and Verdu (PPV) as a benchmark for comparing the performance of AFC at short block lengths. For the AWGN channel, the normal approximation for the achievable rate is given by [23]:

$$R \approx C - \sqrt{\frac{V}{n}} Q^{-1}(\epsilon) + \frac{\log_2 n}{2n}, \quad (15)$$

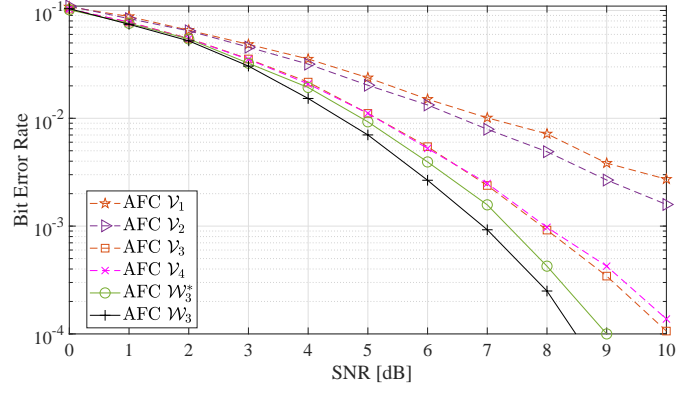


Fig. 4. The BER of an AFC with $n = 8000$, $R_{\text{AFC}} = 0.5$, and optimised weight set \mathcal{W}_3 (Table I), in comparison to previously designed weight sets in the literature (Table II). The weight set $\mathcal{W}_3^* = \{0.5097, 0.4992, 0.4960, 0.4949\}$ was optimised for AFC at $R_{\text{AFC}} = 0.5$ and $\gamma = 5\text{dB}$.

where $C = \frac{1}{2} \log_2(1 + \gamma)$ is the channel capacity, γ is the channel SNR, $V = \log_2^2(e) \frac{\gamma(\gamma+2)}{2(\gamma+1)^2}$ is the channel dispersion, ϵ is the block error rate, and $Q(x) = \frac{1}{\sqrt{2\pi}} \int_x^\infty e^{-\frac{x^2}{2}} dx$ is the standard Q-function.

A. Block Error Rate of AFC at Fixed Rate

We first investigate the block error rate (BLER) performance of precoded AFC truncated at a fixed block length. In particular, we treat AFC as a fixed-rate code in order to investigate the achievable reliability guarantees. This is essential to understand the effect of the precode rate on the overall performance of AFC codes.

Fig. 5 shows the performance of the precoded AFC when a BCH(63,57) code is used as a precode. As can be seen in this figure, the optimized weight set (\mathcal{W}_3 in Table I) outperforms other weight sets previously designed for AFC. The improvement in terms of BLER is consistent when the AFC is operating at different overall rates. Fig. 6 shows the BLER performance of precoded AFC where a BCH(127,57) code is used as a precode. Results are consistent with what we observed in Fig. 5 and that the optimized weight set obtained in this paper outperforms weight sets previously designed for AFC.

Fig. 7 shows the comparison between AFC codes precoded with different BCH codes, i.e., BCH(63,57) and BCH(127,57), where the message length is $k = 57$, and at different overall rates. As can be seen, the AFC code with a low-rate precode achieves a lower BLER. This is mainly because the lower rate precode is more capable of correcting residual errors that AFC is unable to recover, especially when the SNR is low. Fig. 8 shows the same trend at high SNRs, where the lower rate precode performs better in terms of BLER at different rates.

Fig. 7 also shows the performance of precoded AFC using different weight sets. It can be observed that the lower rate precode performs better than the high rate precode when using different weight sets with different degrees. It is important to note that when a high rate precode, i.e., BCH(63,57) is being used, the weight set \mathcal{W}_2 with degree $d_c = 3$ outperforms the other weight sets. However, when the higher rate precode, i.e.,

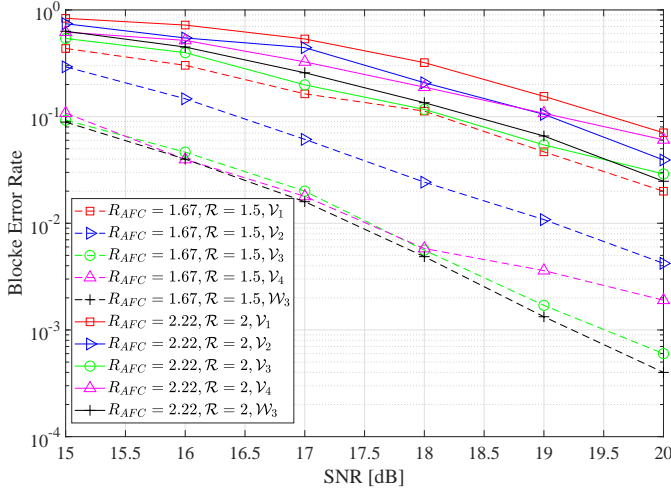


Fig. 5. The BLER of a precoded AFC using weight \mathcal{W}_3 (Table I), in comparison to previously designed weight sets (Table II). The precoder used here is the a BCH(63,57) code.

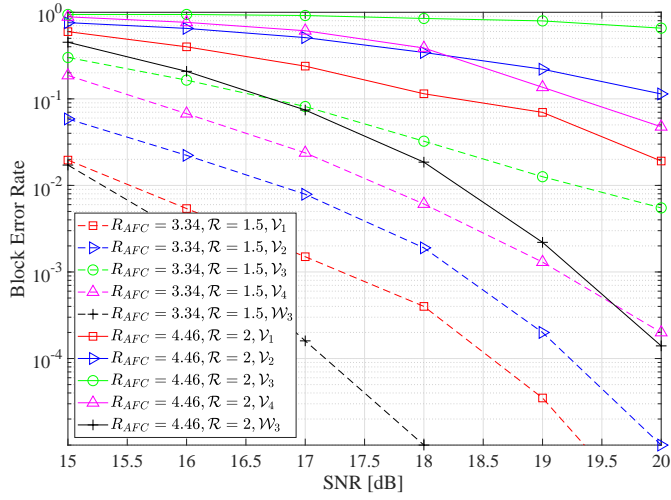


Fig. 6. The BLER of a precoded AFC using weight \mathcal{W}_3 (Table I), in comparison to previously designed weight sets (Table II). The precoder used here is the BCH(127,57) code.

BCH(127,57) is being used, the weight set \mathcal{W}_3 with degree $d_c = 4$ outperforms the other weight sets in different overall rates. This shows that the degree of the AFC code should be chosen carefully and that depends on the precode rate, in order to minimize the block error rate.

Simulation results demonstrate that a similar trend is obtained when using a LDPC code as the precoder, as can be seen in Fig. 9 and Fig. 10. These results further strengthen the statement that we made, which is AFC with a low rate precoder outperforms AFC with the high rate precoder.

B. Achievable Realised Rate

We compare the realised rates achievable by the optimised weights versus previously designed weight sets in Table II. For all simulations, we assumed that the receiver attempts a decoding everytime it receives $\delta = 5$ additional AFC coded symbols. The first decoding attempts occurs when the receiver collects $m_0 = \frac{2k}{\log(1+\gamma)}$ AFC coded symbols, where γ is the channel SNR. The decoder sends an acknowledgment to the

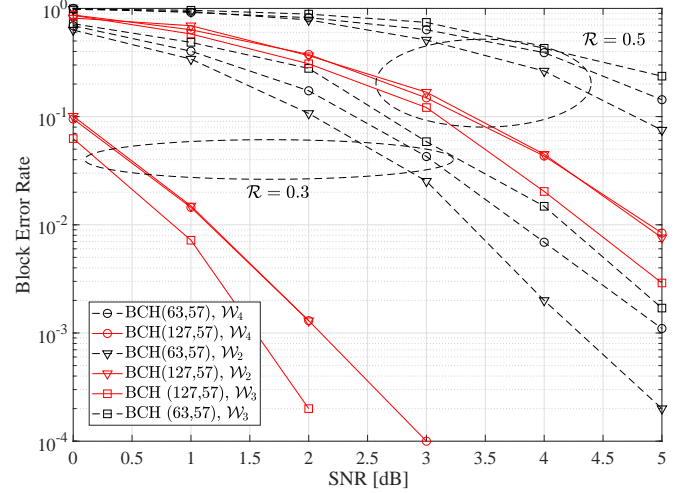


Fig. 7. BLER versus SNR for precoded AFC, when BCH(63,57) and BCH(127,57) are used as precoder, at low SNRs with optimized weight \mathcal{W}_3 .

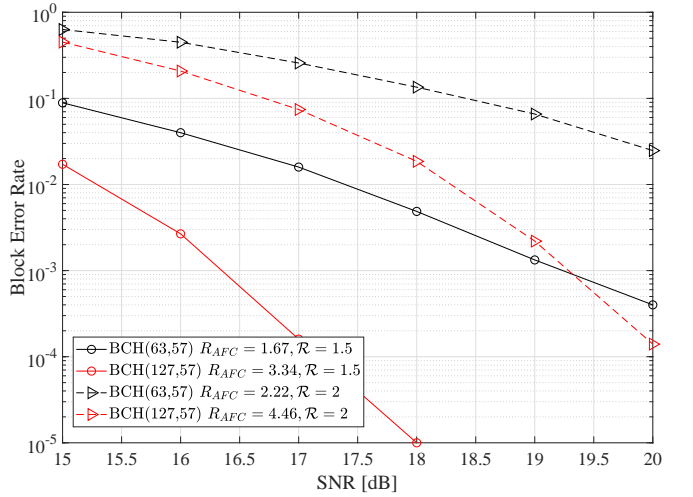


Fig. 8. BLER versus SNR for precoded AFC, when BCH(63,57) and BCH(127,57) are used as precoder, at high SNRs with weight set \mathcal{W}_3 .

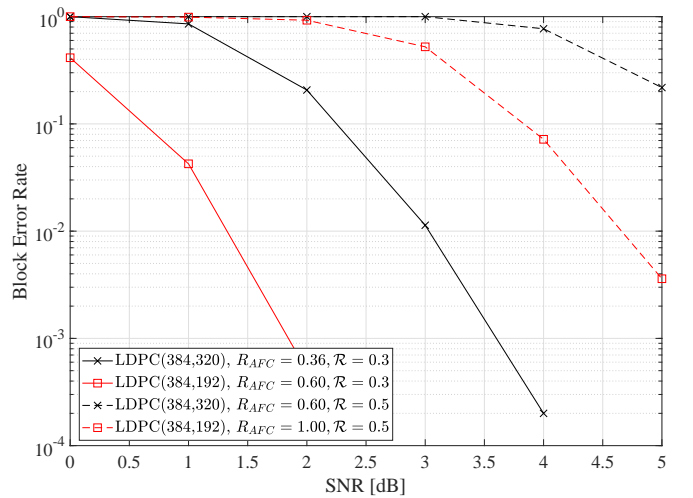


Fig. 9. BLER versus SNR for precoded AFC when LDPC(384,320) and LDPC(384,192) are used as precoder at low SNRs with weight \mathcal{W}_3 .

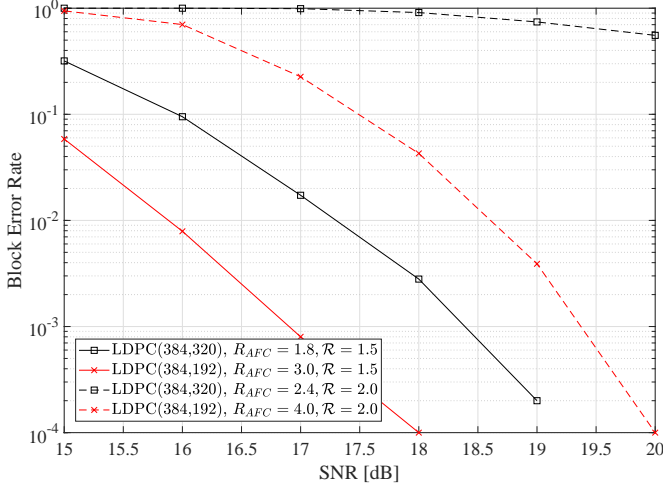


Fig. 10. BLER versus SNR for precoded AFC when LDPC(384,320) and LDPC(384,192) are used as precoder at high SNRs with weight \mathcal{W}_3 .

transmitter when the decoding succeeds and accordingly the transmission is terminated.

Results are shown in Fig. 11. It is clear that our optimised weight set \mathcal{W}_3 is superior in performance to previous AFC weight set designs, with similar degrees, i.e., similar complexity. In particular, for an AFC code precoded with a BCH(63,57), our optimised weight set \mathcal{W}_3 can achieve about 4.35% and 9.68% higher realised rate than weight sets \mathcal{V}_1 and \mathcal{V}_2 , respectively, in the high SNR regime (around 20 dB), and 13.96% and 18.49% higher realised rates, respectively, in the low SNR regime (around 5 dB). When compared with benchmark weight sets \mathcal{V}_3 and \mathcal{V}_4 , the performances of the benchmark weight sets are quite close with our optimised weight set \mathcal{W}_3 , but our optimised weight set still demonstrated superiority compared to benchmark weight sets. Our optimised weight set \mathcal{W}_3 can achieved about 0.84% and 3.37% higher realised rate than weight sets \mathcal{V}_3 and \mathcal{V}_4 , respectively, in the high SNR regime (around 20 dB), and 1.49% and 1.66% higher realised rates, respectively, in the low SNR regime (around 5 dB).

It is important to note that, in theory, the realised rate is defined for the zero-error transmission. However, due to computational limitations, such a realised rate cannot be calculated in practice. Thus, here we assume that the plotted realised rates correspond to block error rates less than 10^{-4} , i.e. for 10^4 messages, no errors are exhibited. Furthermore, since the transmitted block length varies from one frame to the next, we also plot the cumulative distribution function (cdf) of the block length at different SNRs to better understand what latency guarantees AFC can provide. As can be seen in Fig. 12, our optimised code exhibits a smaller variance in the block length than previously designed AFC codes. Thus, our optimised weight set can provide better latency guarantees, particularly for delay sensitive applications with little tolerance for jitters.

Results are shown in Fig. 13, where we consider two precoders a BCH(63,57) code and a BCH(127,57) code. We choose these two precoders such that they have the same

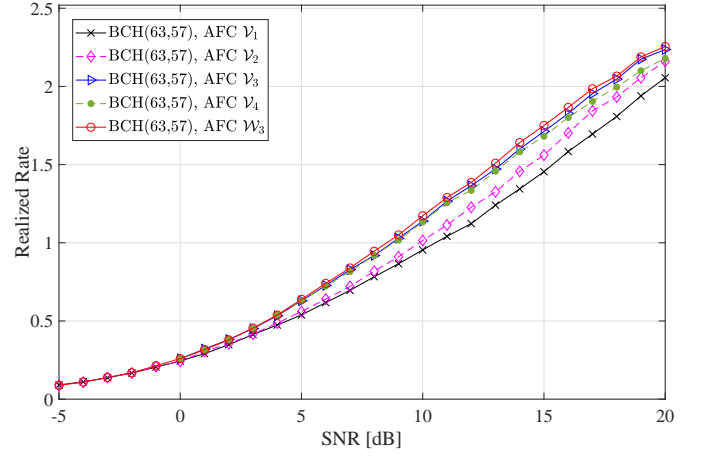


Fig. 11. The realized rates of precoded AFC using our optimised weight set \mathcal{W}_3 (Table I), in comparison to previously designed weight sets in the literature (Table II). The precoder used here is the BCH(63,57) code.

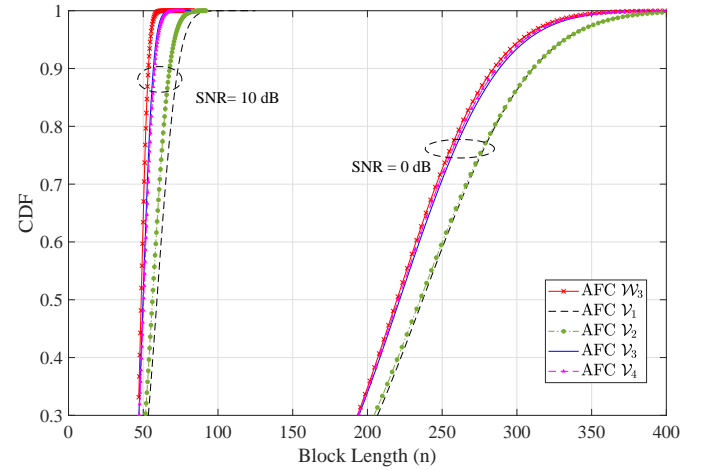


Fig. 12. The cdf of the block length for a precoded AFC using our optimised weight set \mathcal{W}_3 (Table I), in comparison to previously designed weight sets in the literature (Table II). The precoder used here is the BCH(63,57) code.

message length but different rates. For AFC, we use the optimised weight set \mathcal{W}_3 from Table I. As can be seen, the realised rate of AFC with a lower precoder rate is higher than an AFC with a higher rate precoder, over a wide range of SNRs. At SNR of 20 dB, AFC with BCH(127,57) has a gap of 9.57% to the PPV bound compared to AFC with BCH(63,57) which has a gap of 13.68% to the bound. At SNR of 5 dB, AFC with BCH(127,57) is closer to bound, i.e., it has a gap of 7.14% to the bound compared to AFC with BCH(63,57) that has a gap of 9.57% to the bound. Similarly, we observe in Fig. 14 that the CDF of the block length has a smaller variance, i.e. steeper gradient, when the precoder rate is lower. A similar observation was made in [26] for the case of LDPC precoded Raptor codes.

The observation that lower precoder rates have the potential to achieve higher realised rates over a wide range of SNRs is further validated in Fig. 15. In Fig. 15, we use a range of LDPC precoders with different rates and longer block lengths. Results for these medium length blocks show the same trend

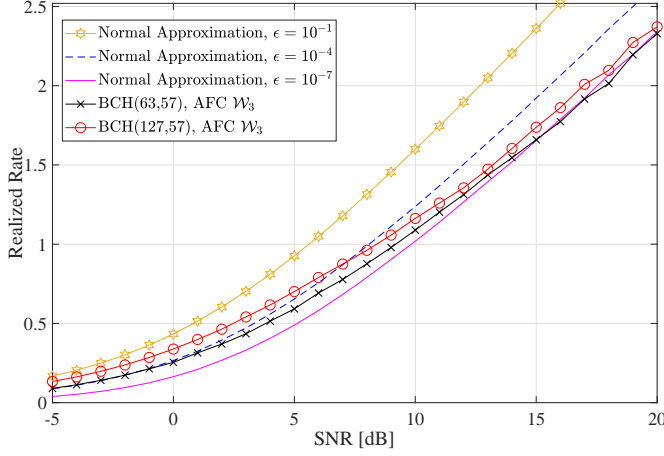


Fig. 13. The realized rates of an AFC precoded with a BCH code using weight set \mathcal{W}_3 .

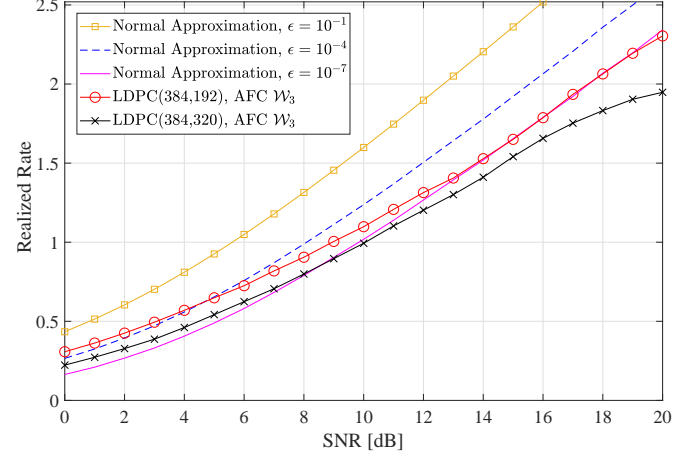


Fig. 15. The realized rates of a precoded AFC using weight set \mathcal{W}_3 (ref. Table I) and different LDPC precoder rates.

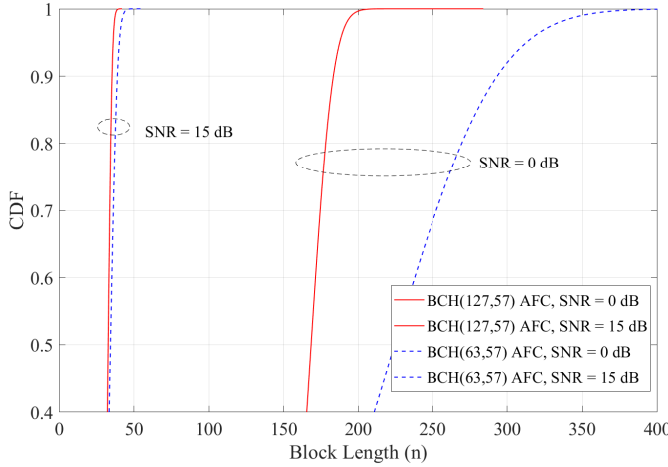


Fig. 14. The cumulative distribution function of the block length of a precoded AFC with weight set \mathcal{W}_3 (ref. Table I) and different precoder rates.

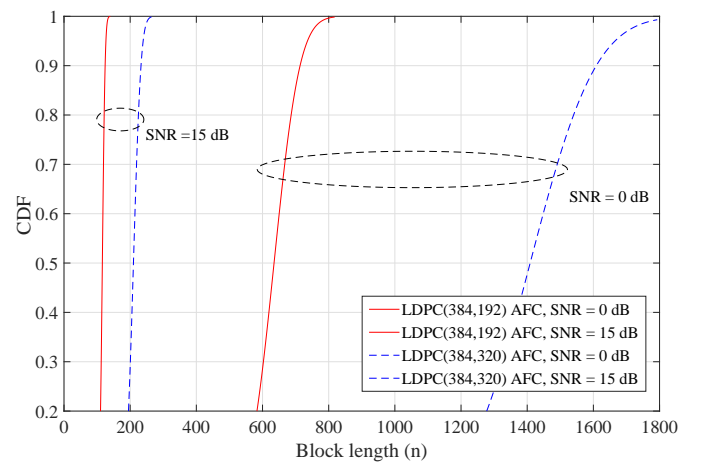


Fig. 16. The cumulative distribution function of the block length of a precoded AFC with weight set \mathcal{W}_3 (ref. Table I) and different LDPC precoder rates.

as those of short blocks in Fig. 13. Furthermore, we also showed that the cdf of block length of the respective AFC with different precoder rates at two regions of SNR in Fig. 16 which demonstrated that lower precoder rate of AFC has steeper gradient compared to higher precoder AFC, further strengthen our claim that lower precoder rate have superior performance compared to higher precoder rate.

For the sake of completion, we would now investigate the performance of the our optimised precoded-AFC using different degrees. It is well established that the degree of the AFC code plays a significant role in its achievable rates, i.e., there is a trade-off between the maximum achievable rate and the allowed encoding/decoding complexity. More specifically, in a noise-free environment, the AFC code can achieve a rate of d_c . However, its decoding complexity increases exponentially with d_c as can be clearly inferred from Section III.

We expect that the check node degree to be the upper bound on the maximum achievable rate when the SNR is sufficiently high. When the BCH(127,57) code is used as the precoder, the achievable rates are plotted in Fig. 17. For medium message lengths, we use the LDPC precoder

due to complexity constraints of the OSD decoder of BCH code. More specifically, when the LDPC(384,192) is used as the precoder the achievable rates are plotted in Fig. 18. We consider three different weight sets, \mathcal{W}_1 , \mathcal{W}_3 , and \mathcal{W}_5 from Table I, with for AFC code with degree $d_c = 2$, $d_c = 4$, and $d_c = 6$, respectively. As can be seen in Fig. 17 and Fig. 18, the AFC code with the larger degree achieves a higher realized rate over a wide range of SNRs.

C. Threshold-based Decoder for BCH

The precoded AFC requires two decoders, i.e, the BP decoder for AFC and the decoder for precoder. The decoding process is carried out in a way that every time that a new set of AFC coded symbols are received, the decoder needs to run both BP and the decoder for precoder. This process will stop only when the decoding succeeds. This leads to a huge complexity at the receiver side and accordingly the decoding time increases dramatically. The problem becomes more challenging when an OSD algorithm is being used for decoding the precoder. When a low rate BCH code is used as the precoder, we

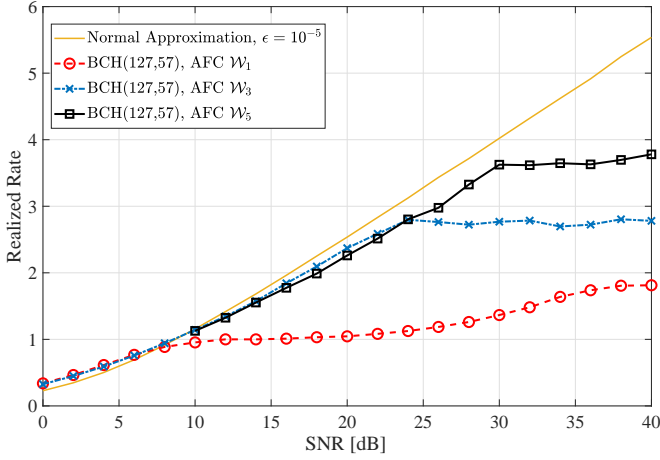


Fig. 17. Realized rate comparison for different degree of optimised weight: W_1, W_2 and W_3 with BCH (127,57)

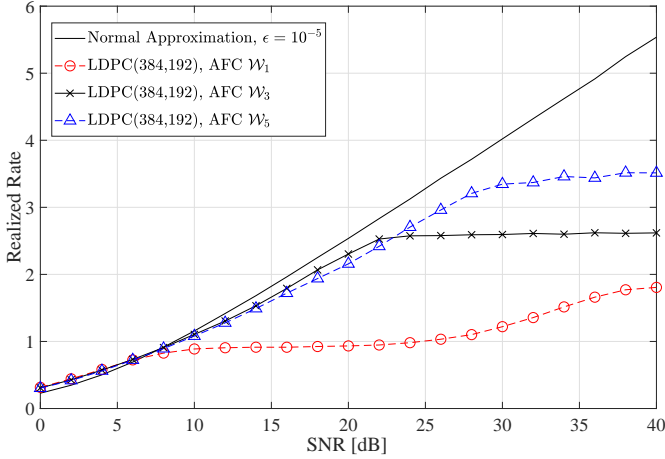


Fig. 18. The realized rates of a precoded AFC using different degrees with LDPC (384,192) as a precoder.

usually need a high-order OSD to be able to achieve a near maximum-likelihood decoding performance. The complexity however increases with $\mathcal{O}(k^\ell)$, where k is the message length and ℓ is the order of OSD. For a code with minimum Hamming distance d_H , order $\ell = \lceil d_H/4 + 1 \rceil$ is asymptotically optimal, i.e., it can achieve near-ML performance [30].

To reduce the decoding complexity, we propose a threshold-based decoding algorithm for the precoded AFC code. In this modified algorithm, we pass the soft information to the precode decoder and perform the algorithm only when the average reliability of the soft information is above a predefined threshold value. Further details of this algorithm can be found in Algorithm 1. Details on how to find the threshold value can be found in [39]. It is important to note that in Step 9 of Algorithm 1, we check CRCs to verify whether the decoding succeeds or not. This is because the output of the OSD is always a valid codeword. Therefore, we need to add CRC bits to verify whether the output of the OSD is the transmitted codeword or not.

In order to show the efficiency of the proposed threshold-based decoder, we evaluate the number of times that we need

Algorithm 1: Threshold-based Decoding for BCH

```

1 Inputs:  $y, G_{\text{pre}}, \delta, m_0, \gamma_{\text{th}}$ 
2 initialization:  $m = m_0$ 
3 while (CRC check fails) do
4   Request for additional  $\delta$  AFC coded symbols
5    $m = m + \delta$ 
6   Perform BP decoding using  $m$  AFC coded symbols
7   Calculate the average LLR of the output of the BP
   decoder,  $\mathbb{E}[|L|]$ 
8   if  $\mathbb{E}[|L|] \geq \gamma_{\text{th}}$  then
9     Perform OSD using  $G_{\text{pre}}$  and  $L$  and check
     CRCs
10  else
11    Go to step 4
12  end
13 end
14 return  $\hat{b}$ 

```

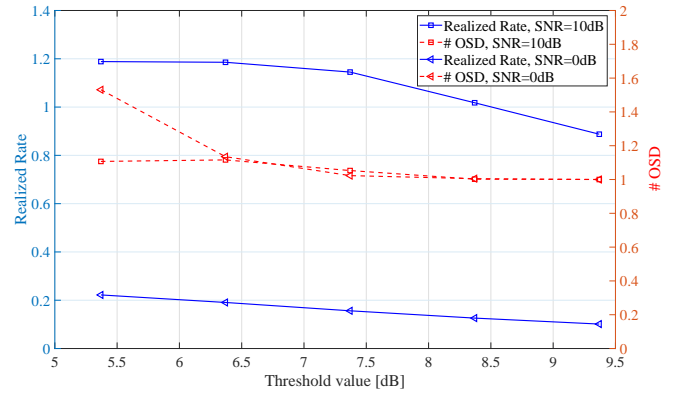


Fig. 19. Number of OSD instances versus the threshold SNR for the BCH-AFC code at different SNRs when BCH(63,57) is used as a precoder.

to run the OSD algorithm versus the threshold SNR. Results are shown in Fig. 19, where the average number of OSD instances and the realized rate are plotted versus the threshold SNR for a precoded AFC at different channel SNRs when BCH(63,57) was used as a precoder. As can be seen in this figure, the number of times that we run OSD is not very sensitive to the threshold value in high SNRs. However, the lower the threshold value, the higher the realized rate. At low SNRs, the threshold value cannot be chosen very small as it significantly increases the number of OSD instances. In fact, one can choose a very low threshold value and get a very high realized rate, but on the other hand the complexity would significantly increase. It is important to note that if the threshold SNR is chosen very low, every time that the receiver receives a new set of AFC symbols, it will run the OSD algorithm, no matter what the reliability of AFC decoder outputs is. The proposed decoder can effectively limit the number of OSD instances to almost 1, when a proper threshold value is considered with a negligible degradation in the realized rate [39].

VI. CONCLUSION

In this paper, we proposed a density evolution (DE) analysis framework for analog fountain codes. In the DE framework, we tracked the evolution of messages exchanged between the variable and check nodes of AFC and characterized their probability density functions. Using the proposed framework, we defined an optimization problem to find the weight set of AFC. Results show that for the asymptotically long message lengths, the optimized weight sets outperform existing weight sets previously designed for AFC. We also studied the design of the precoder for AFC to optimize the performance at short block lengths. We particularly focused on BCH and LDPC codes and showed via simulations that a lower rate precoder can achieve a lower block error rate under the same overall rate and also a higher realized rate over a wide range of signal to noise ratios (SNRs). We further showed that our optimized weight sets outperform existing weight sets in the literature at both low and high SNRs in the short block length regime. We further shed lights on how to reduce the decoding complexity of precoded AFC in the rateless setting. The proposed precoded AFC achieves near optimal performance when the code parameters, such as the code degree, weight set, and precode rate, are chosen properly. The proposed code can be effectively used for rateless transmission of short information sequences, which have applications in many mMTC scenarios. The fact that these codes do not need channel state information at the transmitter side, makes them a strong candidate to reducing significant overhead associated with channel estimation and feedback in mMTC applications.

REFERENCES

- [1] A. Ghosh, A. Maeder, M. Baker, and D. Chandramouli, "5g evolution: A view on 5g cellular technology beyond 3gpp release 15," *IEEE Access*, vol. 7, pp. 127 639–127 651, 2019.
- [2] K. Arora, J. Singh, and Y. S. Randhawa, "A survey on channel coding techniques for 5g wireless networks," *Telecommunication Systems*, pp. 1–27, 2019.
- [3] S. Li, L. Da Xu, and S. Zhao, "5g internet of things: A survey," *Journal of Industrial Information Integration*, vol. 10, pp. 1–9, 2018.
- [4] G. Mei, N. Xu, J. Qin, B. Wang, and P. Qi, "A survey of internet of things (iot) for geohazard prevention: Applications, technologies, and challenges," *IEEE Internet of Things Journal*, vol. 7, no. 5, pp. 4371–4386, 2019.
- [5] H.-M. Wang, Q. Yang, Z. Ding, and H. V. Poor, "Secure short-packet communications for mission-critical iot applications," *IEEE Transactions on Wireless Communications*, vol. 18, no. 5, pp. 2565–2578, 2019.
- [6] P. Schulz, M. Matthe, H. Klessig, M. Simsek, G. Fettweis, J. Ansari, S. A. Ashraf, B. Almeroth, J. Voigt, I. Riedel *et al.*, "Latency critical iot applications in 5g: Perspective on the design of radio interface and network architecture," *IEEE Communications Magazine*, vol. 55, no. 2, pp. 70–78, 2017.
- [7] M. Shirvanimoghaddam, M. S. Mohammadi, R. Abbas, A. Minja, C. Yue, B. Matuz, G. Han, Z. Lin, W. Liu, Y. Li *et al.*, "Short block-length codes for ultra-reliable low latency communications," *IEEE Communications Magazine*, vol. 57, no. 2, pp. 130–137, 2018.
- [8] G. T. 38.802, "Study on new radio access technology physical layer aspects," 2017.
- [9] Y. Kim, Y. Kim, J. Oh, H. Ji, J. Yeo, S. Choi, H. Ryu, H. Noh, T. Kim, F. Sun *et al.*, "New radio (nr) and its evolution toward 5g-advanced," *IEEE Wireless Communications*, vol. 26, no. 3, pp. 2–7, 2019.
- [10] H. Chen, R. Abbas, P. Cheng, M. Shirvanimoghaddam, W. Hardjawana, W. Bao, Y. Li, and B. Vucetic, "Ultra-reliable low latency cellular networks: Use cases, challenges and approaches," *IEEE Communications Magazine*, vol. 56, no. 12, pp. 119–125, 2018.
- [11] M. Luby, "Lt codes," in *The 43rd Annual IEEE Symposium on Foundations of Computer Science, 2002. Proceedings.* IEEE, 2002, pp. 271–280.
- [12] A. Shokrollahi, "Raptor codes," *IEEE transactions on information theory*, vol. 52, no. 6, pp. 2551–2567, 2006.
- [13] B. Bulut, "Experimental analysis and evaluation of raptorq codes for video multicasting over wi-fi," *WIRELESS PERSONAL COMMUNICATIONS*, 2020.
- [14] M. Shirvanimoghaddam, Y. Li, and B. Vucetic, "Adaptive analog fountain for wireless channels," in *2013 IEEE Wireless Communications and Networking Conference (WCNC).* IEEE, 2013, pp. 2783–2788.
- [15] J. Perry, H. Balakrishnan, and D. Shah, "Rateless spinal codes," in *Proceedings of the 10th ACM Workshop on Hot Topics in Networks*, 2011, pp. 1–6.
- [16] X. Wu, M. Jiang, C. Zhao, L. Ma, and Y. Wei, "Low-rate pbrl-ldpc codes for urllc in 5g," *IEEE Wireless Communications Letters*, vol. 7, no. 5, pp. 800–803, 2018.
- [17] N. H. Mahmood, S. Böcker, A. Munari, F. Clazzer, I. Moerman, K. Mikhaylov, O. Lopez, O.-S. Park, E. Mercier, H. Bartz *et al.*, "White paper on critical and massive machine type communication towards 6g," *arXiv preprint arXiv:2004.14146*, 2020.
- [18] Y. Zhang, K. Peng, and J. Song, "A 5g new radio ldpc coded noma scheme supporting high user load for massive mtc," in *2018 IEEE International Conference on Communications (ICC)*, 2018, pp. 1–6.
- [19] G. J. Sutton, J. Zeng, R. P. Liu, W. Ni, D. N. Nguyen, B. A. Jayawickrama, X. Huang, M. Abolhasan, Z. Zhang, E. Dutkiewicz *et al.*, "Enabling technologies for ultra-reliable and low latency communications: From phy and mac layer perspectives," *IEEE Communications Surveys & Tutorials*, vol. 21, no. 3, pp. 2488–2524, 2019.
- [20] W. Rao, Y. Dong, S. Chen, F. Lu, and S. Wang, "An efficient rate compatible modulation with variable weight sets," *IEEE Access*, vol. 6, pp. 5064–5074, 2018.
- [21] F. Lu, Y. Dong, and W. Rao, "A parallel belief propagation decoding algorithm for rate compatible modulation," *IEEE Communications Letters*, vol. 21, no. 8, pp. 1735–1738, 2017.
- [22] R. Abbas, M. Shirvanimoghaddam, T. Huang, Y. Li, and B. Vucetic, "Novel design for short analog fountain codes," *IEEE Communications Letters*, vol. 23, no. 8, pp. 1306–1309, 2019.
- [23] Y. Polyanskiy, H. V. Poor, and S. Verdú, "Channel coding rate in the finite blocklength regime," *IEEE Transactions on Information Theory*, vol. 56, no. 5, p. 2307, 2010.
- [24] K. Zhang, J. Jiao, Z. Huang, S. Wu, and Q. Zhang, "Finite block-length analog fountain codes for ultra-reliable low latency communications," *IEEE Transactions on Communications*, vol. 68, no. 3, pp. 1391–1404, 2020.
- [25] A. Ashikhmin, G. Kramer, and S. ten Brink, "Extrinsic information transfer functions: model and erasure channel properties," *IEEE Transactions on Information Theory*, vol. 50, no. 11, pp. 2657–2673, 2004.
- [26] S. Jayasooriya, M. Shirvanimoghaddam, L. Ong, and S. J. Johnson, "Analysis and design of raptor codes using a multi-edge framework," *IEEE Transactions on Communications*, vol. 65, no. 12, pp. 5123–5136, 2017.
- [27] Z. Cheng, J. Castura, and Y. Mao, "On the design of raptor codes for binary-input gaussian channels," *IEEE Transactions on Communications*, vol. 57, no. 11, pp. 3269–3277, 2009.
- [28] S.-H. Kuo, Y. L. Guan, S.-K. Lee, and M.-C. Lin, "A design of physical-layer raptor codes for wide snr ranges," *IEEE Communications Letters*, vol. 18, no. 3, pp. 491–494, 2014.
- [29] P. Pakzad and A. Shokrollahi, "Design principles for raptor codes," in *2006 IEEE Information Theory Workshop-ITW'06 Punta del Este*. IEEE, 2006, pp. 165–169.
- [30] M. P. Fossorier and S. Lin, "Soft-decision decoding of linear block codes based on ordered statistics," *IEEE Transactions on Information Theory*, vol. 41, no. 5, pp. 1379–1396, 1995.
- [31] D. Baron, S. Sarvotham, and R. G. Baraniuk, "Bayesian compressive sensing via belief propagation," *IEEE Transactions on Signal Processing*, vol. 58, no. 1, pp. 269–280, 2010.
- [32] H. Cui, C. Luo, K. Tan, F. Wu, and C. W. Chen, "Seamless rate adaptation for wireless networking," in *Proceedings of the 14th ACM international conference on Modeling, analysis and simulation of wireless and mobile systems.* ACM, 2011, pp. 437–446.
- [33] T. J. Richardson and R. L. Urbanke, "The capacity of low-density parity-check codes under message-passing decoding," *IEEE Transactions on information theory*, vol. 47, no. 2, pp. 599–618, 2001.
- [34] R. Tanner, "A recursive approach to low complexity codes," *IEEE Transactions on information theory*, vol. 27, no. 5, pp. 533–547, 1981.

- [35] C.-C. Wang, S. R. Kulkarni, and H. V. Poor, "Density evolution for asymmetric memoryless channels," *IEEE Transactions on Information Theory*, vol. 51, no. 12, pp. 4216–4236, 2005.
- [36] E. Dupraz, V. Savin, and M. Kieffer, "Density evolution for the design of non-binary low density parity check codes for slepian-wolf coding," *IEEE Transactions on Communications*, vol. 63, no. 1, pp. 25–36, 2014.
- [37] J. Hou, P. H. Siegel, L. B. Milstein, and H. D. Pfister, "Capacity-approaching bandwidth-efficient coded modulation schemes based on low-density parity-check codes," *IEEE Transactions on Information Theory*, vol. 49, no. 9, pp. 2141–2155, 2003.
- [38] R. Storn and K. Price, "Differential evolution—a simple and efficient heuristic for global optimization over continuous spaces," *Journal of global optimization*, vol. 11, no. 4, pp. 341–359, 1997.
- [39] W. J. Lim, M. Shirvanimoghaddam, R. Abbas, Y. Li, and B. Vucetic, "On the design of analog fountain codes for short packet communications in 5g urllc," in *2019 IEEE 90th Vehicular Technology Conference (VTC2019-Fall)*. IEEE, 2019, pp. 1–5.